Simulation of Possible Future Climate Changes in the 21st Century in the INM–CM5 Climate Model

2 authors:

Some of the authors of this publication are also working on these related projects:

Dynamic modeling of climate changes in the Black Sea area in XXI century View project

Fluctuation-Dissipation, Stochasticity, and Climate-Dependent Subgrid-Scale Parameterizations for Efficient Climate Models View project

Simulation of Possible Future Climate Changes in the 21st Century in the INM-CM5 Climate Model

E. M. Volodin[a], * and A. S. Gritsun[a]

[a]Marchuk Institute of Numerical Mathematics, Russian Academy of Sciences, Moscow, 119333 Russian
***e-mail: volodinev@gmail.com**

Abstract—Climate changes in 2015–2100 have been simulated with the use of the INM-CM5 climate model following four scenarios: SSP1-2.6, SSP2-4.5, and SSP5-8.5 (single model runs) and SSP3-7.0 (an ensemble of five model runs). Changes in the global mean temperature and spatial distribution of temperature and precipitation are analyzed. The global warming predicted by the INM-CM5 model in the scenarios considered is smaller than that in other CMIP6 models. It is shown that the temperature in the hottest summer month can rise more quickly than the seasonal mean temperature in Russia. An analysis of a change in Arctic sea ice shows no complete Arctic summer ice melting in the 21st century under any model scenario. Changes in the meridional streamfunction in atmosphere and ocean are studied.

INTRODUCTION

Forecasting future climate changes is one of the most important applications of climate simulation. This problem can be solved in various ways on different time scales. In this work, we consider probable climate changes in the 21st century associated with changes in the concentrations or emissions of greenhouse and other gases and aerosols associated with human activities.

There are several dozen climate models in the global scientific community, and they differ in the methods used to solve atmosphere and ocean dynamics equations and to parameterize physical processes, spatial resolution, and the presence or absence of certain blocks (for example, atmospheric chemistry, aerosol, and carbon cycle blocks). Climate models are compared every 7–8 years within the CMIP (Coupled Model Intercomparison Project) by means of coordinated experiments with the models. The data of such experiments enter a single database and are processed by different research teams. The processing results are published in scientific papers and in the Reports of the Intergovernmental Panel on Climate Change (IPCC).

Experiments within the 5th phase of CMIP project took place in 2009–2011, and the corresponding 5th IPCC report was published in 2013. The next, 6th phase of the experiments was carried out in 2017–2019. The 6th IPCC report, which should include, among other things, the results of these experiments, is expected to be released in 2022.

The CMIP6 structure was as follows: model groups should first perform the required numerical experiments: a preindustrial experiment for at least 500 years, in which all impacts on the climate system were fixed to 1850; experiments with instant and gradual quadrupling of CO_2 concentration, which allow estimating the equilibrium sensitivity of a model; an experiment with the atmospheric block of a model and a specified state of the ocean surface; and a historical experiment where the climate change for 1850–2014 was simulated and impacts on the climate system were set in accordance with available observations during that time period. After the required experiments, models could participate in different subprojects. One such subproject is the simulation of probable future climate changes in the 21st century according to different scenarios (ScenarioMIP). Numerical experiments, the results of which are discussed in this work, have been performed within this subproject.

The climate is understood as the totality of statistical characteristics of the instantaneous states of the atmosphere, ocean, and other climate system components averaged over a long time period. Therefore, we restrict ourselves to an analysis of some of the most important climate parameters, such as average temperature and precipitation. A more detailed analysis of individual aspects of climate change, such as changes in extreme weather and climate situations, will be the subject of another work. This study is not aimed at a full comparison with the results of other climate models, where calculations follow the same scenarios, since the results of other models have not yet been published in peer-reviewed journals by the time of this writing.

MODEL AND NUMERICAL EXPERIMENTS

The INM-CM5 climate model [1, 2] is used for the numerical experiments. It differs from the previous version, INMCM4, which was also used for experiments on reproducing climate change in the 21st century [3], in the following: an aerosol block has been added to the model, which allows inputting anthropogenic emissions of aerosols and their precursors; the concentrations and optical properties of aerosols are calculated, but not specified, like in the previous version; the parametrizations of cloud formation and condensation are changed in the atmospheric block; the upper boundary in the atmospheric block is raised from 30 to 60 km; the horizontal resolution in the ocean block is doubled along each coordinate; and the software related to adaptation to massively parallel computers is improved, which allows the effective use a larger number of compute cores. The model resolution in the atmospheric and aerosol blocks is $2° \times 1.5°$ in longitude and latitude and 73 levels and, in the ocean, $0.5° \times 0.25°$ and 40 levels. The calculations were performed at supercomputers of the Joint Supercomputer Center, Russian Academy of Sciences, and Moscow State University, with the use of 360 to 720 cores. The model calculated 6−10 years per 24 h in the above configuration.

Four scenarios were used to model the future climate: SSP1-2.6, SSP2-4.5, SSP3-7.0, and SSP5-5.8. The scenarios are described in [4]. The figure after the abbreviation SSP (Shared Socioeconomic Pathway) is the number of the mankind development path (see the values in [4]). The number after the dash means the radiation forcing (W m^{-2}) in 2100 compared to the preindustrial level. Thus, the SSP1-2.6 scenario is the most moderate and assumes rapid actions which sharply limit and then almost completely stop anthropogenic emissions. Within this scenario, greenhouse gas concentrations are maximal in the middle of the 21st century and then slightly decrease by the end of the century. The SSP5-8.5 scenario is the warmest and implies the fastest climate change. Each scenario includes the time series of carbon dioxide, methane, nitrous oxide, and ozone concentrations; emissions of anthropogenic aerosols and their precursors; the concentration of volcanic sulfate aerosol; and the solar constant. The scenarios are recommended for use in the project on comparing CMIP6 (Coupled Model Intercomparison Project, Phase 6, [5]) climate models.

One model experiment was carried out for each of the above scenarios. It began at the beginning of 2015 and ended at the end of 2100. The initial state was taken from the so-called historical experiment with the same model, where climate changes were simulated for 1850−2014, and all impacts on the climate system were set according to observations. The results of the ensemble of historical experiments with the model under consideration are given in [6, 7]. For the SSP3-7.0 scenario, five model runs was performed differing in the initial data taken from different historical experiments. The ensemble of numerical experiments is required to increase the statistical confidence of conclusions about climate changes.

RESULTS

Let us describe some simulation results of climate change in the 21st century. Figure 1 shows the change in the globally averaged surface air temperature with respect to the data of the corresponding historical experiment for 1850−1899. In the warmest SSP5-8.5 scenario, the temperature rises by more than 4° by the end of the 21st century. In the SSP3-7.0 scenario, different members of the ensemble show warming by 3.4°−3.6°. In the SSP2-4.5 scenario, the temperature increases by about 2.4°. According to the SSP1-2.6 scenario, the maximal warming by ~1.7° occurs in the middle of the 21st century, and the temperature exceeds the preindustrial temperature by 1.4° by the end of the century. The results for other CMIP6 models have not yet been published in peer-reviewed journals. However, according to the preliminary analysis (see, e.g., https://cmip6workshop19.sciencesconf.org/data/Session1_PosterSlides.pdf, p.29), the INM-CM5 model shows the lowest temperature increase among the CMIP6 models considered for all the scenarios due to the minimal equilibrium sensitivity to the CO_2 concentration doubling, which is ~2.1° for the current model version, like for the previous version, despite new condensation and cloud formation blocks.

The changes in the surface air temperature are similar for all scenarios; therefore, we analyze the difference between temperatures in 2071−2100 and 1981−2010 under the SSP5-8.5 and SSP1-2.6 scenarios (Fig. 2). The warming is maximal in the Arctic; it reaches 10° and 3°, respectively. Other features mainly correspond to CMIP5 data [8], including the INMCM4 model, which participates in the comparison. The warming on the continents of the Northern Hemisphere is about 2 times higher than the mean, and the warming in the Southern Hemisphere is noticeably less than in the Northern Hemisphere. The land surface is getting warmer than the ocean surface in all the scenarios except SSP1-2.6, because the greenhouse effect is expected to weaken in the second half of the 21st century in this scenario, and the higher heat capacity of the ocean prevents it from cooling as quickly as the land.

The changes in the temperature in individual seasons can noticeably differ from the annual average, and the changes in extreme temperatures can differ from the changes in the averages. The changes in extreme weather and climate events in scenario experiments will be considered in detail in another work. The quality of reproducing the extreme value indices by the INM-CM5 model when reproducing the modern climate is discussed in [9]. Here, we only show how the summer average temperature in 2071−2100 changes as compared to 1980−2010 in Eurasia in the ensemble of
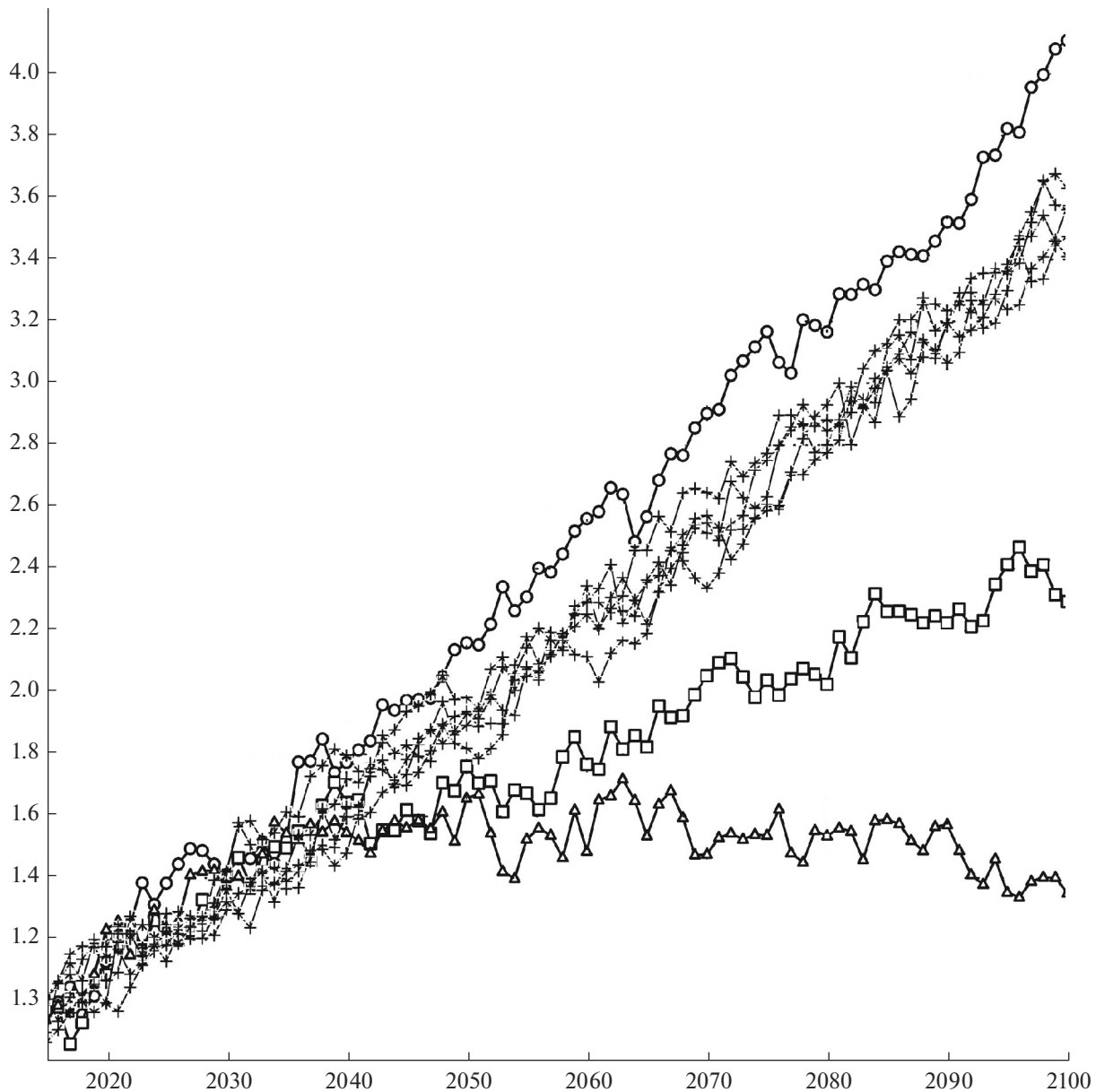
Fig. 1. Changes in the global average surface temperature (K) with respect to the pre-industrial level in experiments according to the SSP1-2.6 (triangles), SSP2-4.5 (squares), SSP3-7.0 (crosses), and SSP5-8.5 (circles) scenarios.

five experiments under the SSP3-7.0 scenario, as well as the temperature of the warmest month over these 30 years. The increase in the summer average temperature is the strongest in southern Europe due more intense soil drying and weaker evaporation. Thirty-year changes in the temperature in the warmest month correspond to an increase in the summer average temperature on the largest area of the globe. However, extremely high temperatures rise faster than the averages in most of Russia (Fig. 3). The probable reason discussed, e.g., in [10] is that the soil usually remains moist, but it can dry sometimes, which, in combination with suitable dynamic conditions, gives a particularly high temperature.

The changes in precipitation in December–February and June–August for the SSP3-7.0 scenario averaged over five members of the ensemble are shown in Fig. 4. All members of the ensemble show an increase in precipitation in the winter in a significant part of middle and high latitudes. In summer, the border between the increase and decrease in precipitation in Eurasia passes mainly around or to the north of 60°. In southern and central Europe, all members of the ensemble show a decrease in precipitation. Precipitation also increases in the region of the summer Asian monsoon, over the equatorial Pacific, due to a decrease in the upwelling and an increase in ocean surface temperature (OST). The distribution of changes in precipi-

(a)

(b)
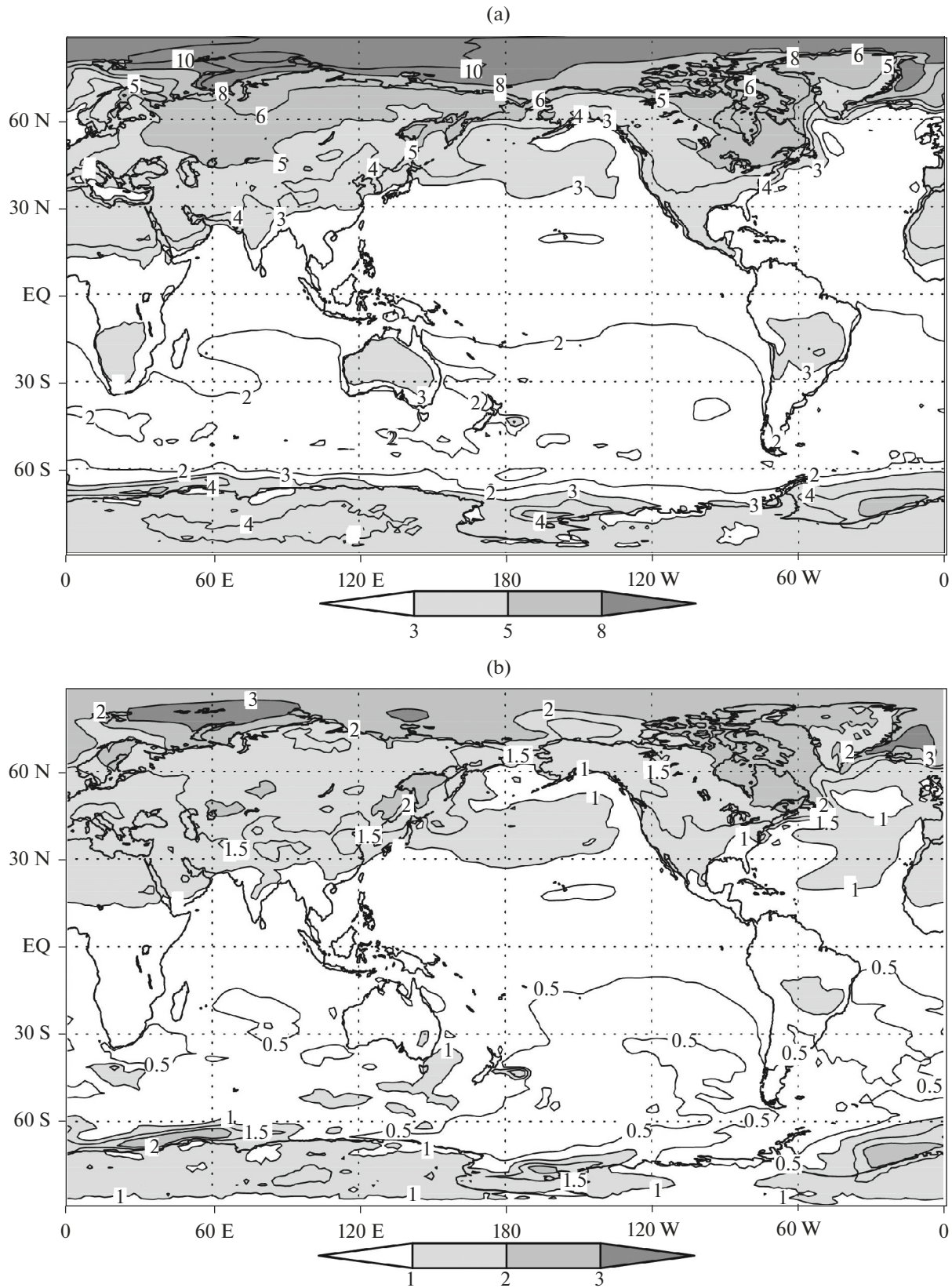
Fig. 2. Differences between the annual average surface air temperatures (K) in 2071−2100 and 1981−2010 for the (a) SSP5-8.5 and (b) SSP1-2.6 scenarios.

(a)

(b)
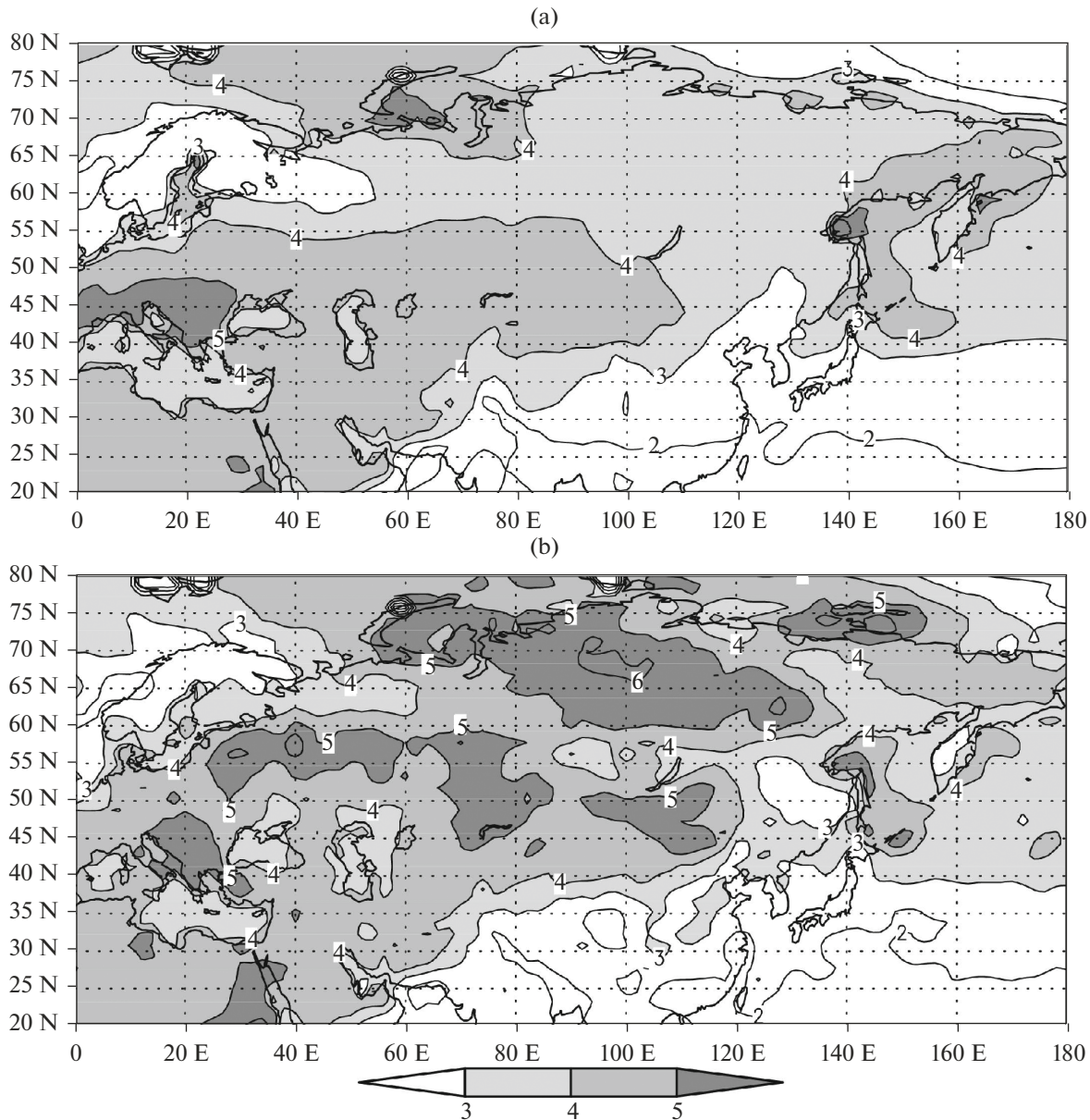
Fig. 3. Differences between the surface temperatures (K) in June−August of 2071−2100 and 1981−2010 for the (a) summer on the average and (b) the warmest months over 30 years.

tation mainly corresponds to that given in [6, Fig. 12.22] for all CMIP5 models.

The change in the Arctic sea ice area in September, when the ocean ice cover is minimal over the year, is of interest. Figure 5 shows the sea ice area in September 2015−2019 to be 4−6 million km² in all experiments, which corresponds to the estimate from observations in [11]. The Arctic sea ice does not completely melt in any of the experiments and under any scenario. However, according to [8, Figs. 12.28 and 12.31], many models participating in CMIP6, where the Arctic ice area is similar to that observed at the beginning of the 21st century, show the complete absence of ice by the end of the 21st century, especially under the RCP8.5 scenario, which is similar to SSP5-8.5. The reason for these differences is the lower equilibrium sensitivity of the INM-CM5 model. Note that the scatter of data between experiments under different scenarios in the first half of the 21st century is approximately the same as between different members of the ensemble under the SSP3-7.0 scenario and becomes larger only after 2070. The sea ice area values are sorted in accordance with the radiative forcing of the scenarios only after 2090. This indicates the large contribution of natural climate variability into the Arctic ice area. In the SSP1-2.6 experiment, the Arctic ice area at the end of the 21st century approximately corresponds to its area at the beginning of the experiment.

(a)

(b)
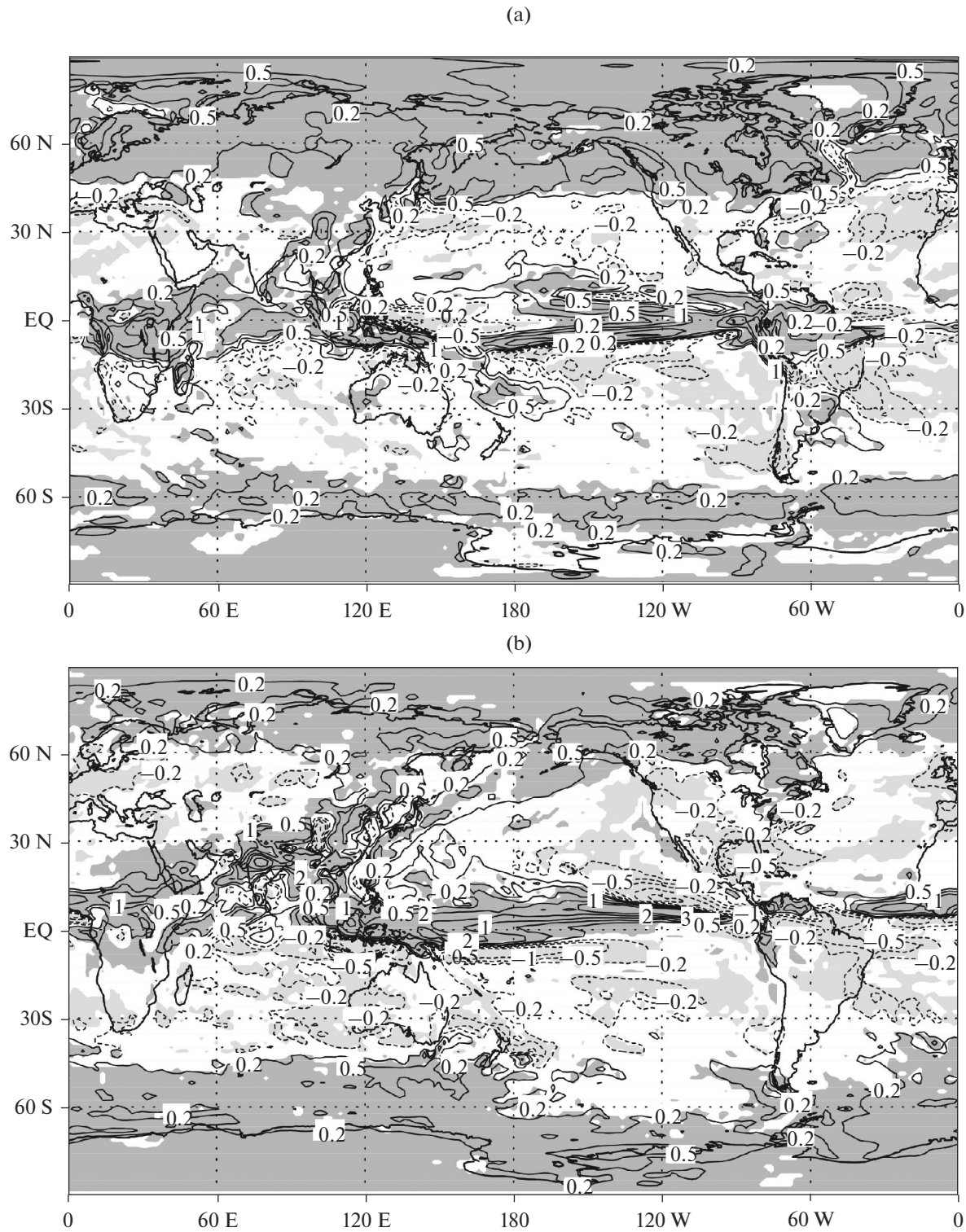
Fig. 4. Changes in precipitation (mm/day) in (a) December−February and (b) June−August 2071−2100 and 1981−2010 averaged over five SSP3-7.0 scenario experiments. Negative isolines are shown by the dashed curve; the regions where all five experiments show changes of the same sign are gray.
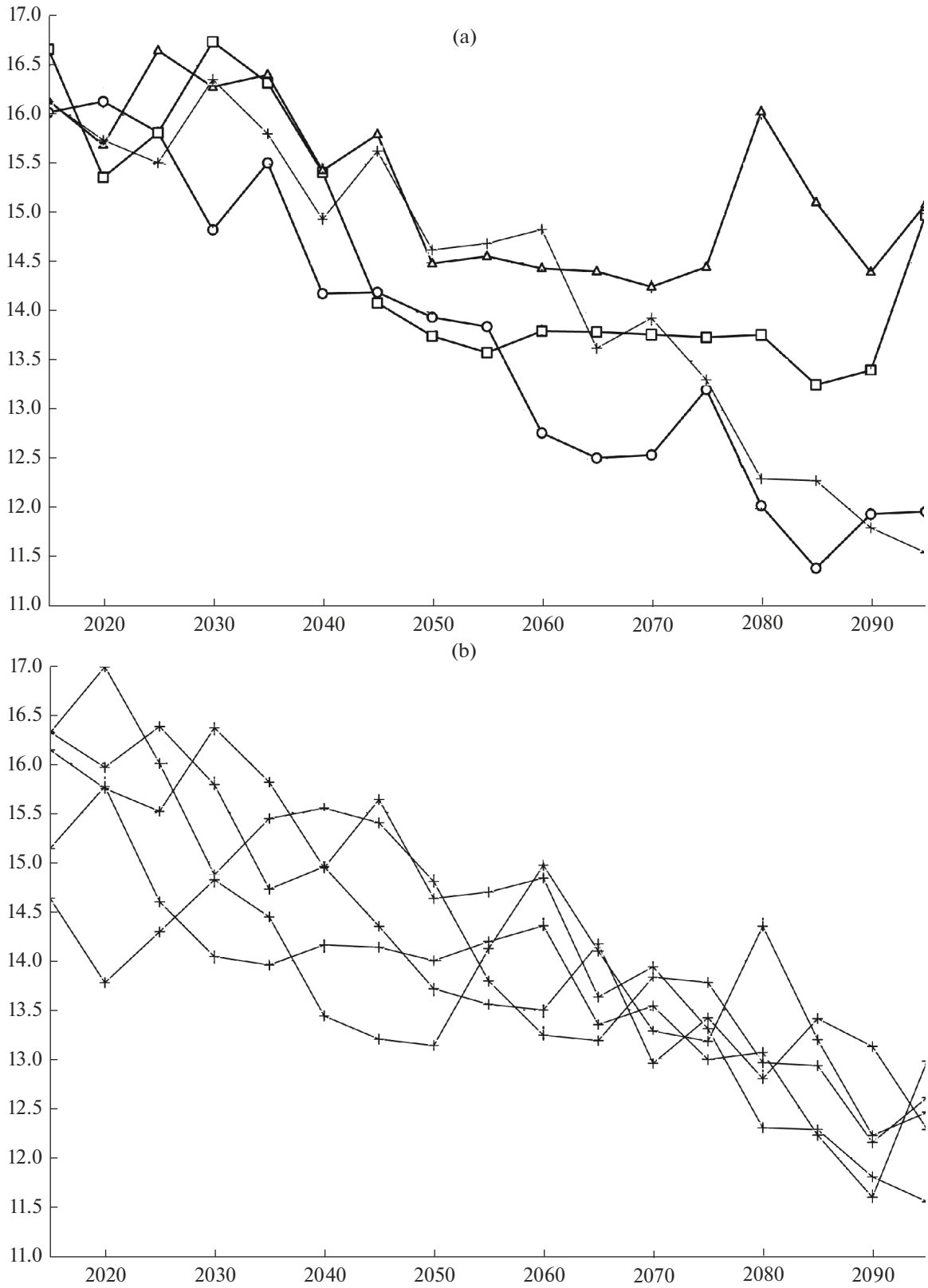
Climate changes can be also traced in the ocean circulation. Figure 6 shows the change in the 5-year averaged intensity of the Atlantic meridional circulation, defined as the maximum of the meridional streamfunction at 32° N. All experiments show a decrease in the intensity of meridional circulation in the 21st century
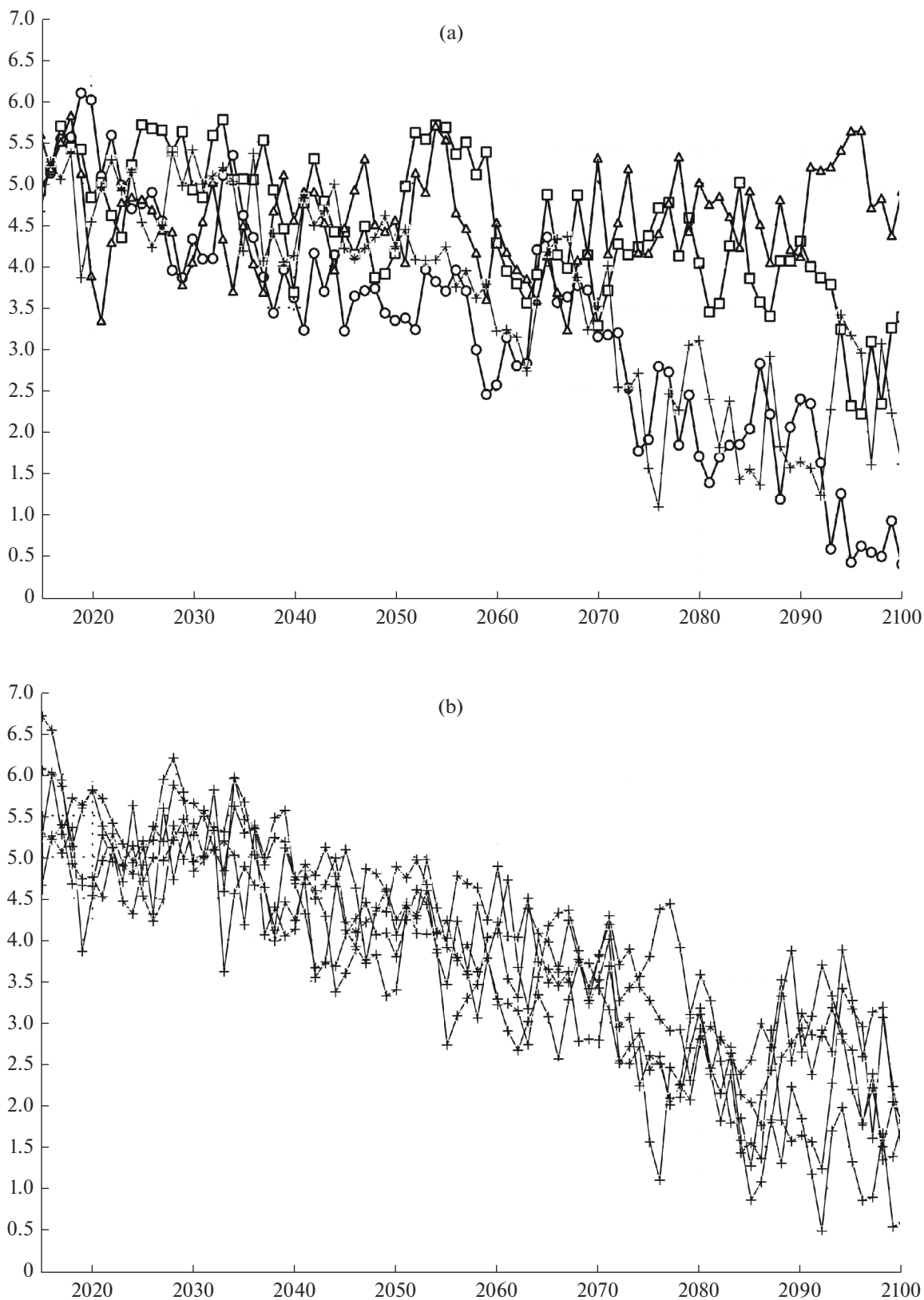
Fig. 5. Arctic ice area (millions km^2) in September: (a) data from experiments under the SSP1-2.6 (triangles), SSP2-4.5 (squares), and SSP5-8.5 (circles) scenarios and the first member of the SSP3-7.0 ensemble (crosses); (b) data of five SSP3-7.0 experiments.

Fig. 6. Five-year averaged intensity of the Atlantic meridional circulation (Sv) defined as the maximum of the meridional stream-function at 32° N: (a) data from experiments under the SSP1-2.6 (triangles), SSP2-4.5 (squares), and SSP5-8.5 (circles) scenarios and the first member of the SSP3-7.0 ensemble (crosses); (b) data from five SSP3-7.0 experiments.

(a)

(b)
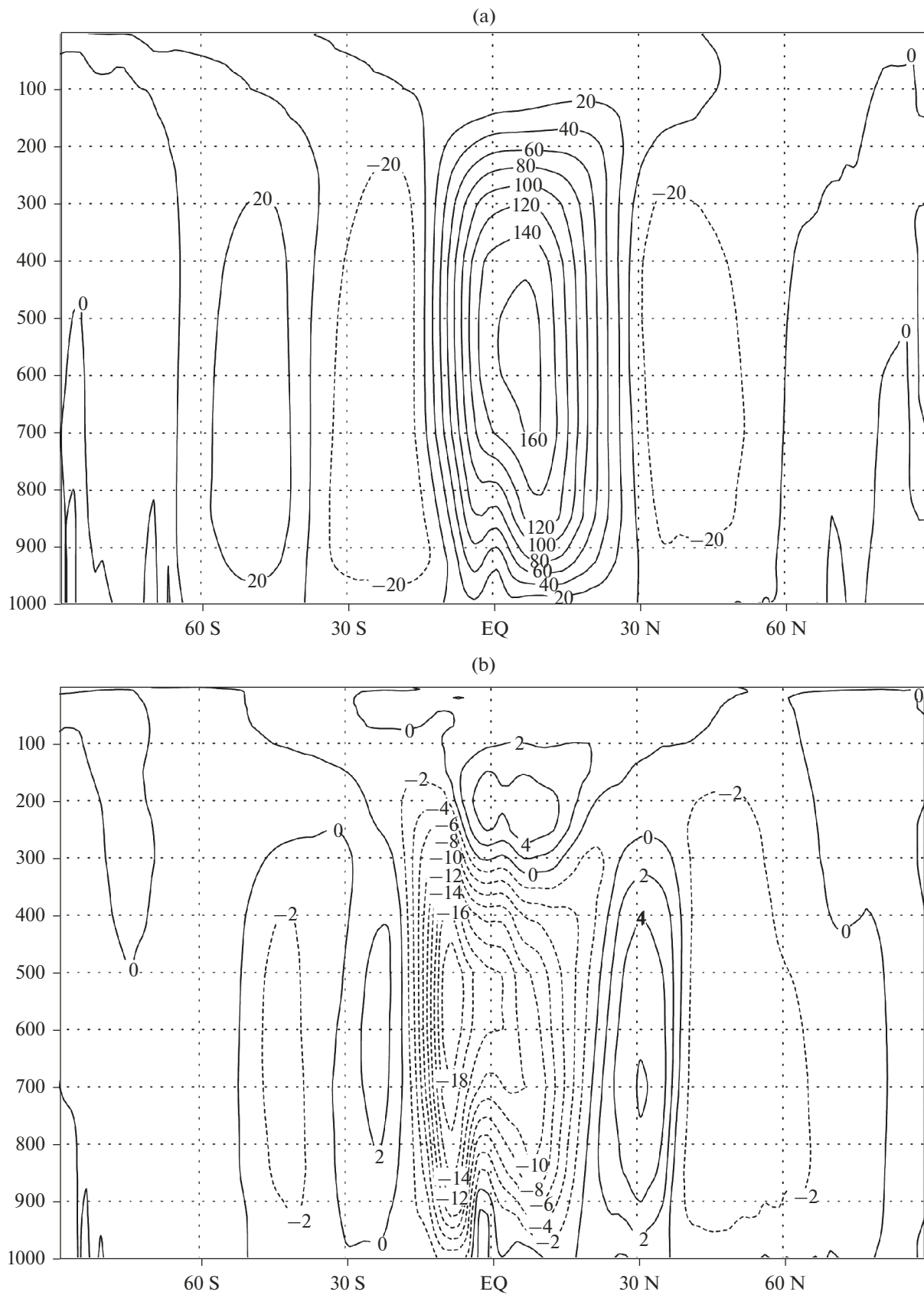
Fig. 7. (a) Meridional streamfunction (10^9 kg s^{-1}) in the atmosphere averaged over December−February 1981−2010; (b) its change in 2071−2100 as compared to 1981−2010.

and natural fluctuations against this decrease. The decrease is about 4.5−5 Sv for the SSP5-8.5 scenario, which is close to values obtained in the CMIP5 models [8, Fig. 12.35] under the RCP8.5 scenario. Under milder scenarios, the weakening of the meridional circulation is less pronounced. The reason for this weakening of the meridional circulation in the Atlantic, as far as we know, is not yet fully understood. In the first half of the 21st century, the scatter of the experimental data for different scenarios, which start with the same initial conditions, is less than the scatter of data of the SSP3-7.0 scenario experimental ensemble, different members of which start from different initial data. This may be evidence of the potential predictability of the meridional circulation intensity for several tens of years from the initial data. At the same time, the scatter of the SSP3-7.0 scenario ensemble significantly decreases by the end of the 21st century, which may mean a decrease in the natural variability in the warmer climate.

Let us mention several other changes in the ocean dynamics which occur by the end of the 21st century, as opposed to the end of the 20th century, in all scenario experiments except for SSP1-2.6.

First, we should note a decrease in the upwelling intensity at the equator in the Pacific, which might be due to a decrease in the trade wind velocity. This increases the OST more strongly than in latitudes farther from the equator and precipitation near the equator.

The Atlantic water inflow into the Arctic Ocean along the west coast of Europe also increases, as does the Arctic water flow into the North Atlantic along the east coast of Greenland. This can be due to both wind exposure (an increase in the North Atlantic Oscillation Index) and a change in the density gradients. In the Atlantic, the surface salinity significantly (by 0.5−1 PSU) increases from the equator to 40° N and similarly decreases in midlatitudes (40°−65° N). It again creases near the ice border in the north of the Barents Sea. These changes in salinity in the model are similar to those in CMIP5 models [8, Fig. 12.34].

The Gulf Stream intensity decreases in the Gulf of Mexico and near the coast of Florida. The Gulf Stream separation point shifts northward. The Kuroshio and the Antarctic circumpolar current intensify.

All these changes in the ocean dynamics during the development of the greenhouse effect, as far as the authors can tell, have no clear explanation in the modern scientific literature and need further research.

The dynamics of the atmosphere also slightly changes due to enhancement of the greenhouse effect. Here, we consider only changes in the meridional circulation during the winter of the Northern Hemisphere (December−February), when these changes are the most pronounced (Fig. 7). The meridional streamfunction shown in Fig. 7 is defined so there is a clockwise movement around the maximum, and counterclockwise around the minimum. In the upper fragment, which shows the intermediate state, the Hadley and Ferrel cells of the Northern and Southern hemispheres are clearly visible. The intensity of the Hadley circulation decreases in both hemispheres in the end of the 21st century, apparently due to an increase in the air moisture content at higher temperatures, which is faster than the increase in precipitation. Therefore, the vertical air stream, which accompanies precipitations, decreases. At the same time, as follows from Fig. 7, the Hadley cell extends upward. In addition, the Hadley circulation cell expands poleward, especially in the Northern Hemisphere. If the zero isoline of the streamfunction is considered its boundary, then the northern boundary shifts poleward by about 1° latitude. The probable cause of this is a change (northward shift) of the momentum fluxes generated by midlatitude Rossby waves, which support the Ferrel circulation. However, to prove this, additional studies are required. The Ferrel cell also shifts northward and slightly strengthens.

The dynamics of the stratosphere also changes. Like in other CMIP5 models ([8, Fig. 12.19]), west winds increase in midlatitudes due to warming of the troposphere and cooling of the stratosphere and a higher tropopause in the tropics than in midlatitudes. This intensifies the vertical wave propagation in midlatitudes and the Brewer−Dobson circulation.

CONCLUSIONS

Numerical experiments have been carried out to reproduce climate changes in the 21st century according to four scenarios of the CMIP6 program [4, 5], including an ensemble of five experiments under the SSP3-7.0 scenario. The changes in the global mean surface temperature are analyzed. It is shown that the global warming predicted by the INM-CM5 model is the lowest among the currently published CMIP6 model data. The geographical distribution of changes in the temperature and precipitation is considered. According to the model, the temperature in the warmest summer month will increase faster than the summer average temperature in Russia.

None of the experiments show the complete melting of the Arctic ice cover by the end of the 21st century. Some changes in the ocean dynamics, including the flow velocity and the meridional streamfunction, are analyzed. The changes in the Hadley and Ferrel circulation in the atmosphere are considered.

ACKNOWLEDGMENTS

REFERENCES

1. E. M. Volodin, E. V. Mortikov, S. V. Kostrykin, V. Ya. Galin, V. N. Lykosov, A. S. Gritsun, N. A. Diansky, A. V. Gusev, and N. G. Yakovlev, "Simulation of modern climate with the new version of the INM RAS climate model," Izv., Atmos. Oceanic Phys. **53,** 142−155 (2017).

2. E. M. Volodin, E. V. Mortikov, S. V. Kostrykin, V. Y. Galin, V. N. Lykossov, A. S. Gritsun, N. A. Diansky, A. V. Gusev, and N. G. Iakovlev, "Simulation of the present-day climate with the climate model INMCM5," Clim. Dyn. **49** (11−12), 3715−3734 (2017).

3. E. M. Volodin, N. A. Diansky, and A. V. Gusev, "Simulation and prediction of climate changes in the 19th to 21st centuries with the Institute of Numerical Mathematics, Russian Academy of Sciences, model of the Earth's climate system," Izv., Atmos. Oceanic Phys. **49** (4), 347−366 (2013).

4. B. C. O' Neill, C. Tebaldi, D. P. van Vuuren, V. Eyring, P. Friedlingstein, G. Hurtt, R. Knutti, E. Kriegler, J.-F. Lamarque, J. Lowe, G. A. Meehl, R. Moss, K. Riahi, and B. M. Sanderson, "The Scenario Model Intercomparison Project (ScenarioMIP) for CMIP6," Geosci. Model Dev. **9,** 3461−3482 (2016).

5. V. Eyring, S. Bony, G. A. Meehl, C. A. Senior, B. Stevens, R. J. Stouffer, and K. E. Taylor, "Overview of the Coupled Model Intercomparison Project Phase 6 (CMIP6) experimental design and organization," Geosci. Model Dev. **9,** 1937−1958 (2016).

6. E. Volodin and A. Gritsun, "Simulation of observed climate changes in 1850−2014 with climate model INM-CM5," Earth Syst. Dyn. **9,** 1235−1242 (2018).

7. E. M. Volodin and A. S. Gritsun, "Nature of the decrease in global warming at the beginning of the 21st century," Dokl. Earth Sci. **482,** 1221−1224 (2018).

8. M. Collins, R. Knutti, J. Arblaster, J.-L. Dufresne, T. Fichefet, P. Friedlingstein, X. Gao, W. J. Gutowski, T. Johns, G. Krinner, M. Shongwe, C. Tebaldi, A. J. Weaver, and M. Wehner, in *Climate Change 2013: The Physical Science Basis. Contribution of Working Group I to the Fifth Assessment Report of the Intergovernmental Panel on Climate Change,* Ed. by T. F. Stocker, D. Qin, G.- K. Plattner, M. Tignor, S. K. Allen, J. Boschung, A. Nauels, Y. Xia, V. Bex, and P. M. Midgley (Cambridge University Press, Cambridge, UK and New York, NY, USA, 2013).

9. E. M. Volodin and M. A. Tarasevich, "Simulation of climate and weather extreme indices with the INM-CM5 climate model," Russ. Meteorol. Hydrol. **43,** 756−762 (2018).

10. E. M. Volodin and A. Y. Yurova, "Summer temperature standard deviation, skewness and strong positive temperature anomalies in the present-day climate and under global warming conditions," Clim. Dyn. **40** (5−6), 1387−1398 (2013).

11. J. C. Comiso and F. Nishio, "Trends in the sea ice cover using enhanced and compatible AMSR-E, SSM/I, and SMMR data," J. Geophys. Res.-Oceans **113** (C2), S07 (2008).
https://doi.org/10.1029/2007JC004257

Translated by O. Ponomareva